Daily to Decadal Sea Surface Temperature Variability Driven by State-Dependent Stochastic Heat Fluxes

Philip Sura, Matthew Newman, and Michael Alexander

NOAA-CIRES Climate Diagnostics Center, Boulder, Colorado

February 17, 2005

Submitted to *Journal of Physical Oceanography*

Corresponding author address:
Philip Sura
NOAA-CIRES Climate Diagnostics Center, R/CDC1
325 Broadway, Boulder, CO 80305-3328
Phone: (303) 497-4426, Fax: (303) 497-6449
E-Mail: Philip.Sura@noaa.gov

Abstract

The classic Frankignoul-Hasselmann hypothesis for sea surface temperature (SST) variability of an oceanic mixed layer assumes that the surface heat flux can be simply parameterized as noise induced by atmospheric variability plus a linear temperature relaxation rate. It is suggested here, however, that rapid fluctuations in this rate, as might be expected for example due to gustiness of the sea surface winds, are large enough that they cannot be ignored. Such fluctuations cannot be fully modeled by noise that is independent of the state of the SST anomaly itself. Rather, they require the inclusion of a state-dependent (that is, multiplicative) noise term, which can be expected to impact both persistence and the relative occurrence of high amplitude anomalies.

As a test of this hypothesis, daily observations at several Ocean Weather Stations are examined. Significant skewness and kurtosis of the distributions of SST anomalies is found, which is shown to be consistent with a multiplicative noise model. This model (counter-intuitively) implies that the multiplicative noise increases the persistence, predictability, and variance of midlatitude SST anomalies. The effect is strongest on annual and longer timescales and may, therefore, be important to understand and model interannual and interdecadal SST and related climate variability.

1 Introduction

The typical timescale of atmospheric variability is considerably shorter than the typical timescale of sea surface temperature (SST) variability. As a result, the effect of atmospheric forcing of SST anomalies T' can be represented by a simple stochastic model of the oceanic mixed layer,

$$\frac{dT'}{dt} = -\lambda T' + \xi \tag{1}$$

(Hasselmann 1976; Frankignoul and Hasselmann 1977, hereafter FH), where λ is a rate coefficient representing the transfer of heat from the slowly evolving mixed layer heat anomaly, and ξ is Gaussian white-noise representing surface heat fluxes due to rapidly varying weather fluctuations. The e-folding timescale of SST variability is thus $\tau = 1/\lambda$. Such a simple univariate linear system has been surprisingly successful in describing much of the variability of anomalous midlatitude SSTs (e.g., Frankignoul and Hasselmann 1977; Reynolds 1978; Blaauboer et al. 1982; Hall and Manabe 1997).

This classical stochastic view implies that SST anomalies obey a Gaussian distribution. Indeed, *monthly averaged* SST anomalies are nearly Gaussian. Yet we might expect them to be Gaussian because of the Central Limit Theorem (e.g., Gardiner 2004; Paul and Baschnagel 1999), i.e., the Gaussianity may be due solely to the averaging procedure and not to any particular dynamical process. In fact, as we will show, observations from Ocean Weather Stations (OWSs) reveal that probability distribution functions (PDFs) of *daily averaged* SST anomalies are actually significantly non-Gaussian.

The presence of non-Gaussianity suggests the possible importance of nonlinearity to the

evolution of SST anomalies, appearing to contradict the FH paradigm. However, if this nonlinearity also acts on a very short timescale, then the FH paradigm may only require a small adjustment. Suppose the linear coefficient in (1) contains a rapidly varying component; that is, $\lambda = \bar{\lambda} + \lambda'$, where $\bar{\lambda}$ is constant but λ' varies rapidly; note that the time mean of λ' is zero. Such rapid fluctuations in the feedback coefficient might be expected, for example, if it has a dependence upon not just a constant or slowly varying wind speed, but also upon the gustiness of the winds. Then we might also approximate λ' as white-noise. However, unlike the noise term ξ which is independent of T', a stochastically fluctuating λ' would result in a second noise term $\lambda' T'$ which depends upon the SST anomaly itself. This state-dependent noise is also known as multiplicative noise. A system driven with such multiplicative noise has two characteristics of interest here. First, in general it will have a non-Gaussian PDF, even though the deterministic portion of (1) is linear. Second, although the autocorrelation function for T' remains an exponential, the multiplicative noise acts to effectively increase the time scale τ through a phenomenon known as noise-induced drift, which occurs because the time mean of the multiplicative noise term, $\langle \lambda' T' \rangle$, is not zero. For a mathematically more advanced discussion, see, for example, Gardiner (2004); Kloeden and Platen (1992), and see Penland (2003a,b) for a related discussion focusing on climate dynamics.

In this paper we present a simple univariate stochastic model of midlatitude SST anomalies that accounts for rapid fluctuations in surface heat fluxes, such as might result from the gustiness of sea surface winds. The parameters of this model are determined from OWS data whose non-Gaussian probability distribution functions (PDFs) are described in section 2. In section 3 we justify a noise component of λ through a scale analysis of wind-driven surface

heat flux, as parameterized by simple heat flux bulk formulae. This hypothesis is then tested in section 4 by estimating both linear and nonlinear models from data. Furthermore, the nonlinear model is used to examine the impact of multiplicative noise on the predictability and low-frequency variability of SST anomalies. Finally, section 5 provides a summary and discussion.

2 PDFs of daily averaged SST

To re-examine the effect of stochastic weather fluctuations on anomalous SSTs, we first analyze the PDFs of daily averaged SST anomalies obtained from Ocean Weather Station records [see Dinsmore (1996) for a brief history of Ocean Weather Stations and Diaz et al. (1987) for climatological summaries]. Table 1 lists the stations analyzed, their locations, and the time periods of data availability. We restrict our study to locations where univariate linear stochastic theory provides a good fit to observed anomalous SST variability: P, N, and V in the North Pacific, and K in the North Atlantic.

2.1 Data

Daily SST anomalies were determined as follows. First, daily averages were calculated from the raw 3-hourly data. Then the climatological monthly averages were estimated. A daily climatology was constructed by linear interpolation using these monthly averages as base points. Finally, daily anomalies were calculated by subtracting the daily climatology from the mean daily values.

We analyzed the resulting full-year SST anomaly timeseries. To account for possible effects of the annual cycle we analyzed extended summer (May-October) and extended winter (November-April) subsets as well.

2.2 Probability Density Functions

PDFs are a useful measure to examine the dynamics of stochastic systems. In particular, deviations from Gaussianity, or anomalous statistics, can shed light on the underlying dynamics (e.g., Peinke et al. 2004; Sura et al. 2005). PDFs can be estimated using different techniques. The easiest way is to calculate the normalized histogram by binning the data. This is a non-parametric method because no assumptions are made of the functional form of the PDF. Non-parametric methods are normally used as a reliable first-order PDF estimate when there is no reasonable physical justification for a particular distribution. For a parametric estimation of a PDF one specifies the functional form of the PDF in advance, and the parameters of the PDF are then determined by a Maximum Likelihood Estimate (MLE). The parametric distribution we use is the skew t-distribution, a skewed and kurtosed alternative to the normal distribution which is capable of adapting very closely to skewed and heavy-tailed data (Azzalini and Capitanio 2003; Jones and Faddy 2003). We use both methods here.

In the following section, all discussed deviations from Gaussianity are significant at least at the 95% confidence level, with large amplitude deviations significant at the 99% confidence level, as determined by the Monte-Carlo method employed in, e.g., Sura et al. (2005).

2.3 Ocean Weather Station P

Of all the Ocean Weather Stations, OWS P may be best suited for linear univariate stochastic theory (Hall and Manabe 1997). It has a long high-quality record, the El Niño-Southern Oscillation (ENSO) signal is relatively weak there (e.g., Alexander et al. 2002), and it is located far from strong currents.

The PDFs of full-year daily SST anomalies, related Gaussian distributions, and anomalies (deviations from Gaussianity) at OWS P are shown in Fig. 1. In Fig. 1a the PDF (steps) is calculated as a normalized histogram, whereas in Fig. 1b the PDF (solid line) is calculated as a MLE to a skew t-distribution. Comparison in either case to the related Gaussian distribution (dashed lines) shows that the PDF has a strong peak, weak flanks, and heavy tails relative to a Gaussian distribution (i.e., the PDF is kurtosed). Furthermore, the PDF is slightly skewed. The skew t-distribution captures all the important features of the histogram: the strong peak, weak flanks, heavy-tails, and the skew.

2.4 Other Ocean Weather Stations

Hall and Manabe (1997) have shown that while over most of the world ocean anomalous SST variability is consistent with the simple FH model, there are a few regions where this stochastic theory cannot be applied. Near strong boundary currents like the Gulf Stream and the Kuroshio (and both their extensions, the North Atlantic and the North Pacific currents) mesoscale eddies enhance SST variability at high-frequencies. Furthermore, in the northern North Atlantic, large scale variations of the thermohaline ocean circulation are responsible

for much of the low-frequency variations. And, of course, regions with sea-ice are excluded as well.

After analyzing data from the remaining stations, we find that, in agreement with Hall and Manabe (1997), there are four stations with long records where the autocorrelation functions (and the spectra) can be modeled with univariate red noise: P, N, and V in the North Pacific, and K in the North Atlantic. These stations are all in midlatitudes and far away from strong currents. The PDFs (full year, extended summer and winter) of SST anomalies at these stations are shown in Fig. 2 (we only show the skew t-distributions in Fig. 2; the histograms have a similiar shape). The PDFs at OWSs K and N are qualitatively similar to the PDF at OWS P (Fig. 1), although their deviations from Gaussianity are somewhat larger. OWS V shows a slightly different behavior: the PDFs have similar kurtosis as the other stations, but the skew has the opposite sign. In all cases, similar deviations from Gaussianity is present in both the winter and summer subsets.

To summarize, the non-Gaussianity at OWS P is not unique but a general feature at OWSs where linear stochastic theory can be applied. Furthermore, the non-Gaussianity does not appear strongly seasonally dependent, suggesting that the full-year daily SST anomaly record can be used to study anomalous SST variability.

3 Extending the Frankingnoul-Hasselmann null hypothesis

Having shown that daily SST anomalies at OWS P, and other stations where univariate stochastic theory is applicable, obey a non-Gaussian distribution, we next show how rapidly fluctuating winds could act to produce similar non-Gaussianity. The model developed is a straightforward extension of the classic FH stochastic SST anomaly model, in which we add a stochastic process to the constant feedback coefficient.

3.1 The basic mixed layer equations

The simplest model for midlatitude SSTs assumes a well mixed and horizontally homogeneous layer of constant depth h and temperature T in contact with the overlying atmosphere, but isolated from the layers below the thermocline. For the sake of simplicity, all effects of horizontal advection and salinity are ignored as well. Then the local heat budget equation can be written as (see, e.g. Frankignoul and Hasselmann 1977)

$$\frac{dT}{dt} = \frac{f(T, T_a, q, |\mathbf{U}|, R)}{h} \quad , \tag{2}$$

where f denotes the total heat flux through the air-sea interface, which depends on the SST T, air temperature T_a, humidity q, wind speed $|\mathbf{U}|$, and the net radiation R. Neglecting the radiation flux, the bulk formula for the heat flux f is

$$f = \frac{\rho_a C_a}{\rho_w C_w} C_H (1 + B)(T_a - T)|\mathbf{U}| \quad , \tag{3}$$

where C_H is the bulk transfer coefficient of the latent and sensible heat flux, B is the inverse Bowen ratio (ratio of latent to sensible heat flux), ρ_w and ρ_a are the densities of sea-water and air, and C_w and C_a are the specific heats (at constant pressure) of sea-water and air.

For small temperature anomalies ΔT a Taylor expansion of the heat flux f with respect to $T = T_0 + \Delta T$ yields

$$\frac{d}{dt}(T_0 + \Delta T) = \frac{1}{h}\left[f(T_0) + \frac{\partial f}{\partial T}\Big|_{T_0}\Delta T\right] \quad . \tag{4}$$

Assuming that the evolution of the temperature T_0 is balanced by the time mean of $f(T_0) = \langle f\rangle(T_0) + f'(T_0)$, that is $dT_0/dt = \langle f\rangle(T_0)/h$, and defining $\Delta T \equiv T'$ the equation for the SST anomaly T' becomes:

$$\frac{dT'}{dt} = \frac{f'(T_0)}{h} + \frac{1}{h}\frac{\partial f}{\partial T}\Big|_{T_0}T' \quad . \tag{5}$$

As in FH variations in the atmospheric temperature T_a, the inverse Bowen ratio B, and the transfer coefficient C_H are ignored. That is, we assume that heat flux variability is only due to wind speed variability. This is a reasonable approximation in our simple framework, since heat flux anomalies are strongly related to wind speed anomalies (e.g., Ronca and Battisti 1997; Alexander and Scott 1997). The wind speed is split into a mean $\langle|\mathbf{U}|\rangle$ and a deviation from the mean $|\mathbf{U}|'$, so that the mean heat flux $\langle f\rangle(T_0)$ depends upon $\langle|\mathbf{U}|\rangle$ and the heat flux deviation $f'(T_0)$ depends upon $|\mathbf{U}|'$. Then the anomalous heat flux f' and the heat flux derivative $\partial f/\partial T$ become

$$f'(T_0) = \frac{\rho_a C_a}{\rho_w C_w} C_H(1+B)(T_a - T_0)|\mathbf{U}|' \tag{6}$$

and

$$\frac{\partial f}{\partial T}\Big|_{T_0} \equiv \left\langle\frac{\partial f}{\partial T}\right\rangle + \left(\frac{\partial f}{\partial T}\right)' = -\frac{\rho_a C_a}{\rho_w C_w} C_H(1+B)\left[\langle|\mathbf{U}|\rangle + |\mathbf{U}|'\right] \quad , \tag{7}$$

where $\partial f/\partial T$is split into a mean heat flux derivative $\langle \partial f/\partial T \rangle = -(\rho_a C_a)(\rho_w C_w)^{-1} C_H (1 + B)\langle |\mathbf{U}| \rangle$ and an anomalous heat flux derivative $(\partial f/\partial T)' = -(\rho_a C_a)(\rho_w C_w)^{-1} C_H (1+B)|\mathbf{U}|'$. Note that f' is a function of only $|\mathbf{U}|'$, whereas $\partial f/\partial T$ is a function of both $\langle |\mathbf{U}| \rangle$ and $|\mathbf{U}|'$.

3.2 Scaling the equation

To see if a multiplicative noise term is necessary, we first scale the terms in Eqs. (5), (6), and (7). Using typical parameters for the conditions at OWS P (see Table 2) we obtain $f'(T_0)/h = O(0.2 \text{ K day}^{-1})$, $h^{-1}\langle \partial f/\partial T \rangle T' = O(0.1 \text{ K day}^{-1})$, and $h^{-1}(\partial f/\partial T)' T' = O(0.05 \text{ K day}^{-1})$. Note that the relative importance of $h^{-1}\langle \partial f/\partial T \rangle T'$ and $h^{-1}(\partial f/\partial T)' T'$ is solely determined by the ratio of the mean wind speed $\langle |\mathbf{U}| \rangle$ to the strength of the wind speed anomaly $|\mathbf{U}|'$. As this ratio is only about 2 to 1 throughout the midlatitude storm tracks (e.g., Monahan 2005) the effect of wind fluctuations on SST anomalies may come through the variability of not only the anomalous heat flux f' but also the anomalous heat flux derivative $(\partial f/\partial T)'$.

3.3 Neglecting the anomalous heat flux derivative $(\partial \mathbf{f}/\partial \mathbf{T})'$: Modeling SST anomalies with additive noise

In the stochastic SST model introduced by FH, the anomalous heat flux derivative was neglected. The heat flux term f'/h [see Eq. (6)] is parameterized as Gaussian (additive) white-noise η [scaled by the parameter σ; see Eq. (8) below]. In other words, it is assumed that $|\mathbf{U}|'$ can be approximated by Gaussian white-noise. This assumption is reasonable since daily wind speed anomalies are almost uncorrelated and have a distribution that is

nearly Gaussian. For example, at OWS P wind speed anomalies are almost uncorrelated after 2–3 days (Fig. 3a) and deviations from Gaussianity are relatively small (Fig. 3b). Then, treating the term $h^{-1}\partial f/\partial T$ [see Eq. (7)] as a constant parameter $\lambda = h^{-1}\langle \partial f/\partial T\rangle = -h^{-1}(\rho_a C_a)(\rho_w C_w)^{-1} C_H (1+B)\langle |\mathbf{U}|\rangle$, FH derived the familiar stochastic differential equation (SDE):

$$\frac{dT'}{dt} = -\lambda\, T' + \sigma\, \eta \quad , \tag{8}$$

with the Gaussian white-noise η satisfying $\langle \eta(t)\rangle = 0$ and $\langle \eta(t)\eta(t')\rangle = \delta(t-t')$. This is the SDE of a univariate Ornstein-Uhlenbeck process, also called damped Brownian motion. When λ is determined from observations, (7) results in the familiar red-noise spectrum of T' in close agreement with observations. However, the PDF of an Ornstein-Uhlenbeck process is strictly Gaussian and, therefore, not consistent with the results of section 2. Thus, the classical stochastic model of midlatitude SST variability should be improved to explain the non-Gaussianity of observed SST anomalies. Here we improve the stochastic model by including the anomalous heat flux derivative $(\partial f/\partial T)'$.

3.4 Including the anomalous heat flux derivative $(\partial \mathbf{f}/\partial \mathbf{T})'$: Modeling SST anomalies with multiplicative noise

The scaling analysis of section 3.2 suggests that $h^{-1}\partial f/\partial T$ should not be a constant parameter. Moreover, to be consistent $|\mathbf{U}|'$ should be a stochastic process both in Eqs. (6) and (7). That is, the anomalous heat flux derivative $(\partial f/\partial T)'$ is parameterized as multiplicative noise, since it is the product of a slowly varying quantity (T') and a rapidly varying quantity

($|\mathbf{U}|'$). Therefore, we consider the following SDE for T':

$$\frac{dT'}{dt} = -\lambda T' + \sqrt{2M}\, T'\, \eta_M + \sqrt{2D}\, \eta_D \tag{9}$$

with Gaussian white-noise satisfying

$$\langle \eta_M(t)\eta_M(t')\rangle = \delta(t-t') \ , \ \langle \eta_D(t)\eta_D(t')\rangle = \delta(t-t')\,. \tag{10}$$

D and M are constants governing the strength of the additive and multiplicative noise terms. Note that the actual noise amplitudes are $\sqrt{2D}$ and $\sqrt{2M}$; this definition is solely used for later mathematical convenience.

As was discussed in the introduction, multiplicative noise acts to lengthen the observed decorrelation timescale of T'. The autocorrelation function $\langle T'(t)T'(s)\rangle$ is given by (Sakaguchi 2001; Anteneodo and Tsallis 2003)

$$\langle T'(t)T'(s)\rangle = \frac{D}{\lambda - 2M} \exp\left(-(\lambda - M)|t-s|\right) \qquad . \tag{11}$$

As is the case with purely additive noise ($M = 0$), the autocorrelation decays exponentially. However, the decorrelation timescale is now $\tau = (\lambda - M)^{-1} = \lambda_{eff}^{-1}$. That is, the noise-induced drift is M, so that stronger multiplicative noise *increases* the persistence of midlatitude SST anomalies. The spectrum of SST anomalies $S(\omega)$ can be calculated by Fourier-transforming the autocorrelation function (11):

$$S(\omega) = \frac{D(\lambda - M)}{(\lambda - 2M)} \ \left(\omega^2 + (\lambda - M)^2\right)^{-1} \qquad . \tag{12}$$

In addition, the multiplicative noise acts to produce a non-Gaussian stationary PDF of T':

$$p(T') = \Theta(D + MT'^2)^{-\Pi} \tag{13}$$

(Sakaguchi 2001; Anteneodo and Tsallis 2003) where $\Pi = (\lambda_{eff} + 2M)/2M$. The normalization constant Θ is given by:

$$\Theta = \frac{M^{1/2} D^{\Pi - 1/2}}{\beta(1/2, \Pi - 1/2)} = \frac{M^{1/2} D^{\Pi - 1/2} \Gamma(\Pi)}{\Gamma(1/2)\Gamma(\Pi - 1/2)} \tag{14}$$

where $\beta(x, y)$ is the beta-function, and $\Gamma(x)$ is the gamma-function: $\beta(x, y) = \Gamma(x)\Gamma(y)/\Gamma(x + y)$. Having $p(T')$ the moments of T' can be calculated. The first (mean) and the third moment (skew) are zero because the problem is symmetric with respect to $T' = 0$. The second moment (variance) is

$$\langle T'^2 \rangle \equiv \int_{-\infty}^{\infty} T'^2 p \, dT' = \frac{D}{\lambda_{eff} - M} \,, \tag{15}$$

and the fourth moment (kurtosis) is

$$\langle T'^4 \rangle \equiv \int_{-\infty}^{\infty} T'^4 p \, dT' = \frac{3D^2}{\lambda_{eff}^2 - 4\lambda_{eff} M + 3M^2} \,. \tag{16}$$

4 Inverse Stochastic Models of SST Anomalies

In the following we determine stochastic models for anomalous SST variability from data. First (in section 4.1) we estimate the parameters of the linear multiplicative noise model [Eq. (9)]. Second (in section 4.3) we estimate a more general nonlinear stochastic model from data to test the validity of the linear model. Furthermore, we use the nonlinear model to explore the impact of multiplicative noise on the predictability and the low-frequency vatiability of SST anomalies.

4.1 Linear inverse model

The parameters in (9) can be estimated from data by first determining the variance $\langle T'^2 \rangle$, the kurtosis $\langle T'^4 \rangle$, and the effective damping λ_{eff} from the observed autocorrelation function. For OWS P these are ($\pm$ one standard error): $\lambda_{eff} = 0.0157 \pm 0.0002$ day^{-1}, $\langle T'^2 \rangle = 0.71 \pm 0.01$ K^2, and $\langle T'^4 \rangle = 1.78 \pm 0.06$ K^4. Then M and D can be found from the two equations [Eqs. (15) and (16)]. The nonlinear (quadratic) equations for the noise parameters M and D have only one physically consistent solution: $M = 0.0011 \pm 0.0003$ day^{-1} and $D = 0.0104 \pm 0.0002$ K^{2}day^{-1}. The noise amplitudes in Eq. (9) are therefore: $\sqrt{2M} = 0.0469 \pm 0.0064$ day$^{-1/2}$ and $\sqrt{2D} = 0.1442 \pm 0.0014$ K day$^{-1/2}$.

Fig. 4 shows the distribution $p(T')$ as defined by Eqs. (13) and (14) for $\lambda_{eff} = 0.0157$ day^{-1}, $D = 0.0104$ K^{2}day^{-1} , and $M = 0.0011$ day^{-1}, the related Gaussian distribution, and the corresponding deviation from Gaussianity. The multiplicative noise causes the distribution to have a more pronounced peak, weaker flanks, and heavier tails compared to a Gaussian distribution. That is, the multiplicative noise increases the kurtosis of the distribution. Thus, this simple model is able to explain the basic (neglecting the skew) non-Gaussian structure of the observed PDF (Fig. 1).

The effect of multiplicative noise in the linear stochastic model upon the spectrum of SST variability [Eq. (12)] at OWS P is shown in Fig. 5. The spectrum with pure additive noise ($\lambda = 0.0168$ day^{-1}, $D = 0.0104$ K^{2}day^{-1}, and $M = 0$ day^{-1}) is indicated by the dashed line, and the spectrum with multiplicative noise included ($\lambda = 0.0168$ day^{-1}, $D = 0.0104$ K^{2}day^{-1}, and $M = 0.0011$ day^{-1}) is indicated by the solid line. Multiplicative noise

enhances low-frequency SST variability of anomalous SST variability by about 25% (even as the total noise variance increases only by about 8%).

4.2 Testing the multiplicative white-noise model

When we fit Eq. (9) to the data, we are making two assumptions: that the forcing is white, and that it is multiplicative. Neither, however, need be true to get a good linear fit of the autocorrelation function. These assumptions can be tested in a straightforward manner. The effective drift λ_{eff} estimated from data can be used to 'predict' T' after a time step Δt: $T'(t+\Delta t) = -\lambda_{eff}\, T'_{obs}(t)\, \Delta t + T'_{obs}(t)$. If the white-noise assumption is correct the difference between the observed value $T'_{obs}(t+\Delta t)$ and the predicted value $T'(t+\Delta t)$ should equal the white-noise forcing. The autocorrelation function of the residual $r \equiv T'_{obs}(t+\Delta t) - T'(t+\Delta t)$ is shown in Fig. 6a. The residual is almost uncorrelated after one time step (one day), justifying the white-noise approximation.

The PDF of the residual (Fig. 6b) is very close to an exponential distribution (straight line in logarithmic plot) and is thus highly non-Gaussian. To test whether this residual represents multiplicative white-noise or merely non-Gaussian additive noise, we executed a numerical experiment in which the model (8), with $\lambda_{eff} = 0.0158$ day^{-1} and additive noise whose distribution is the same as the residual, is integrated forward for 500000 days. The resulting PDF differs from that in Fig. 4 and is nearly Gaussian.

This result is not entirely surprising, since a simple scaling argument also shows that non-Gaussian additive noise alone has no significant effect on the distribution of SST anomalies.

Since $\lambda \sim [O(0.02)\,\mathrm{day}^{-1}]$ while $f'/h \sim [O(0.2)\,\mathrm{K\ day}^{-1}]$, $dT'/dt \approx f'/h$ so $T' \approx \sum_j f_j/h\,\Delta t$, and the Central Limit Theorem applies. In other words, for sufficiently small λ, non-Gaussian additive noise will result in a Gaussian distribution of SST anomalies T'. Thus, the non-Gaussianity of the observed PDF implies that the residual represents multiplicative noise.

4.3 A nonlinear stochastic inverse model

In the previous sections we showed that the linear model can explain the observed kurtosis of SST anomalies, but it cannot explain the observed skew. In this section we consider the most general (nondimensional) form of the univariate SDE that governs the evolution of SST anomalies,

$$\frac{dT'}{dt} = A(T') + B(T')\eta \quad , \tag{17}$$

where $A(T')$ represents all slow processes and $B(T')\eta$ represents the stochastic approximation to the fast nonlinear processes. The Gaussian white-noise η satisfies $\langle \eta(t) \rangle = 0$ and $\langle \eta(t)\eta(t') \rangle = \delta(t-t')$. Note that the deterministic dynamics in $A(T')$ are no longer required to be linear and that $B(T')\eta$ now represents both multiplicative and additive noise. As in the linear case, the multiplicative noise produces a drift, such that $A_{eff} = A + (1/2)\,B\,(\partial B/\partial T')$ (e.g., Gardiner 2004).

Because the individual records from the OWSs are too short to accurately determine the nonlinear stochastic model of anomalous SST variability, we concatenated the normalized records from stations where stochastic theory is applicable, and where the skew has the same sign: K in the North Atlantic, and P, N in the North Pacific (see the discussion in section 2). Note that the concatenated timeseries is nondimensional. The resulting PDF is shown

in Fig. 7. As in the case of OWS P (Fig. 1), the PDF is calculated both as a normalized histogram (Fig. 7a) and as a MLE to a skew t-distribution (Fig. 7b). The PDF of the concatenated record has the same structure as the record from OWS P: it is clearly kurtosed and slightly skewed. Note, however, that the deviations from Gaussianity are larger for the concatenated record than for the OWS P record.

The nonlinear model can also be estimated from the data. The effective drift $A_{eff}(T')$ is found by using its finite-difference definition

$$A_{eff}(T') = \lim_{\Delta t \to 0} \frac{1}{\Delta t} \langle T'(t + \Delta t) - T' \rangle |_{T'(t)=T'} \tag{18}$$

(e.g., Siegert et al. 1998; Friedrich et al. 2000; Gradišek et al. 2000; Sura and Barsugli 2002; Sura 2003; Sura and Gille 2003); the result is shown in Fig. 8a (the error bars indicate $\pm$ one standard error). Note that $A_{eff}(T')$ is almost linear and acts to damp anomalous SSTs. Therefore, a linear approximation is justified, as shown by the solid line: $A_{eff}(T') \approx -0.023\, T'$. We next use the PDF $p(T')$ and the effective drift $A_{eff}(T')$ to determine $B(T')$ from the Fokker-Planck equation (see Sura et al. 2005) corresponding to (17):

$$B(T') = \left(\frac{2}{p(T')} \int_{-\infty}^{T'} [A_{eff}(x') p(x')]\, dx' \right)^{1/2} . \tag{19}$$

The estimated noise $B(T')$ for the SST anomalies is shown by the solid line in Fig. 8b; the dotted line in Fig. 8b shows the optimal linear multiplicative noise obtained by fitting the variance and the kurtosis of the PDF (Fig. 7) to the linear SDE (9). The linear multiplicative noise qualitatively captures the main features of $B(T')$. However, there is clearly a nonlinear component to $B(T')$, since $B(T')$ is not symmetric with respect to $T' = 0$, and the curvature (second derivative) of $B(T')$ is larger on the right hand side of the minimum at $T' \approx 0.8$

than on the left hand side (Fig. 8b). Therefore, the noise is stronger for positive SST anomalies than it is for negative anomalies, resulting in the observed skew. Note that the weak departure of $A(T')$ from linearity contributes very little to the observed skew and kurtosis.

We next use the effective drift $A_{eff}(T')$ and the noise $B(T')$ to determine the real deterministic drift $A(T')$. Shown in Fig. 9 are the noise-induced drift $(1/2)\,B\,(\partial B/\partial T')$, the real deterministic drift A, and the effective drift A_{eff}. Note that the noise-induced drift is almost linear and, as in the linear system discussed in the previous section, acts to undamp the system. That is, the results of the linear model are confirmed by the nonlinear model.

4.4 Predictability

We might expect that, due to the increase in persistence that results from the noise-induced drift, SST anomalies driven by multiplicative noise might be potentially more predictable than those driven by additive noise. The situation may, however, be complicated by increased uncertainty resulting from the multiplicative noise itself. To assess this issue we compute a simple measure of predictability, the anomaly correlation of an ensemble mean perfect forecast with observations, which can be written as:

$$\rho_\infty(\tau) = \frac{S(\tau)}{\sqrt{S(\tau)^2 + 1}} \tag{20}$$

where $S(\tau) \equiv s(\tau)/\sigma(\tau)$ is the signal-to-noise ratio and τ is the forecast lead (e.g., Sardeshmukh et al. 2000; Newman et al. 2003b). Here the signal $s(\tau)$ is the ensemble mean, and the noise $\sigma(\tau)$ is the ensemble standard deviation. $\rho_\infty(\tau)$ is the expected skill of a perfect

model in which the signal is determined as the mean of an infinite-member ensemble [see Sardeshmukh et al. (2000) or Newman et al. (2003b) for a more detailed discussion].

Two different stochastic models are compared the full multiplicative noise model (17), and a second "additive noise" model containing the same deterministic term $A(T')$ but in which only additive noise, scaled to yield the (unit) variance of the concatenated SST anomaly timeseries, is used. That is, the variances of SST anomalies are the same in both the additive and the multiplicative noise models. Fig. 10 shows the forecast lead at which expected forecast skill ρ_∞ falls below 0.5, as a function of initial condition for the additive (dashed line) and the multiplicative noise model (solid line). In this simple example, multiplicative noise increases the lead time of skillful forecast from large negative SST anomalies (larger than one standard deviation) by about 5–10 days. Skill from positive anomalies is actually slightly worse, as in general skill from positive anomalies is lower than skill of similar amplitude negative anomalies. This result suggests that the anomalous heat flux derivative, parameterized as multiplicative noise, has a significant impact on the predictability of SST anomalies.

4.5 Spectra

Finally, the impact of multiplicative noise upon the low-frequency variability of SST anomalies is demonstrated by numerically integrating two different stochastic models, with and without multiplicative noise. Both models have the same deterministic dynamics $A(T')$, but the additive noise model uses pure additive noise (the strength of the additive noise is given by the minimum of $B(T')$), whereas the multiplicative noise model uses the full multiplica-

tive noise term $B(T')$ (Fig. 8b). The spectra of both models are shown in Fig. 11. The spectrum with pure additive noise is indicated by the dashed line, and the spectrum with multiplicative noise included is indicated by the solid line.

Multiplicative noise enhances the low-frequency variability of anomalous SST variability by about 100% (even as the total noise variance increases only by about 30%). The linear model for OWS P showed that the multiplicative noise enhanced the low-frequency variability of anomalous SST variability by about 25%, whereas the total noise variance increased by about 8% (Fig. 5). Why is there such a difference between OWS P and the concatenated record? The non-Gaussianity of the concatenated SST anomaly record is larger than the non-Gaussianity at OWS P, resulting in correspondingly stronger multiplicative noise. As confirmed by a linearization of $A(T')$ and $B(T')$, the spectral difference between OWS P and the concatenated record is mainly due to the different strengths of the multiplicative noises and not to nonlinear effects. That means, the linear approximations of $A(T')$ and $B(T')$ are very good representations (neglecting the skew) of the underlying physical processes. Again, the results of the linear model are confirmed by the nonlinear model.

5 Summary and Discussion

In this paper we showed that distributions of daily SST anomalies at several Ocean Weather Stations are non-Gaussian. Broadly speaking, the distributions have a stronger peak, weaker flanks, and heavier tails than the related Gaussian distributions. We suggested that this observed non-Gaussianity can be understood with a simple extension to the FH stochastic

model of midlatitude SST anomalies, accounting for the effect of rapid variability of surface winds (parameterized as noise) upon both the surface heat flux and the surface heat flux derivative (with respect to SST). The latter effect results in multiplicative noise and has been ignored in many simple stochastic models (e.g., Frankignoul and Hasselmann 1977).

Our key point is that inclusion of this multiplicative noise term allows the FH model to qualitatively reproduce not only an exponential autocorrelation function, but also the main features of the observed distributions of SST anomalies. The model (counterintuitively) also predicts that this multiplicative noise can increase the persistence, predictability, and low-frequency variability of midlatitude SST anomalies. That is, part of the observed autocorrelation of SST anomalies is due to the noise-induced drift.

Given that the effect of multiplicative noise appears somewhat stronger in the inverse model than the simple heuristic model of section 3, there are likely other sources of multiplicative noise that should be considered. Earlier studies considering multiplicative noise forcing of SST (Alexander and Penland 1996; Neelin and Weng 1999) suggested that changes in the SST anomaly could produce changes in atmospheric variability and thus in the forcing term f'. Note that in our study, multiplicative noise forcing of the mixed layer exists even if the atmosphere is *not* sensitive to changes in midlatitude SST. Still, if atmospheric noise in (9) is a function of T', for example if $\sqrt{2M}\,T'$ is replaced with $\sqrt{2M(T')}\,T'$, then the multiplicative noise might no longer be linear. This is one possible source of the small deviation of $B(T')$ from linearity seen in Fig. 8b.

We have employed a simple approach to focus upon basic effects of multiplicative noise in the FH framework. Clearly, though, any significant dependence of atmospheric noise

upon the SST anomaly could necessitate the use of a stochastic coupled model, such as that employed by Barsugli and Battisti (1998). They suggested that coupling enhances the thermal variance in the ocean and the atmosphere by reducing the anomalous air-sea temperature difference. How surface wind variability impacts their model is a focus of our current research; note that they considered only thermal noise, whereas changes in wind variability due to the SST anomaly may require non-local feedbacks.

We have also not considered forcing of midlatitude oceans, particularly the North Pacific, by the atmospheric bridge that results from ENSO (e.g., Alexander et al. 2002; Newman et al. 2003a). Noise-induced drift could enhance the mean response to ENSO forcing (Sardeshmukh et al. 2001), particularly where ENSO also increases high-frequency atmospheric variability (Smith and Sardeshmukh 2000; Compo et al. 2001). For multivariate systems, external forcing can result in a skewed PDF even if the multiplicative noise term is linear (Sura et al. 2005).

Our results demonstrate that the high-frequency variability of boundary-layer winds and related heat fluxes are crucial for understanding low-frequency anomalous SST variability. That is, we see a scale interaction between the fast wind induced heat flux variability and the slow SST variability. This scale interaction has implications for atmospheric forcing employed in ocean models, suggesting that the high-frequency variability of boundary layer winds and related surface fluxes must be accurately simulated to correctly model low-frequency variability of SSTs.

Acknowledgments. This work was partially supported by a grant from NOAA CLIVAR/Pacific.

References

Alexander, M. A., I. Blade, M. Newman, J. R. Lanzante, N.-C. Lau, and J. D. Scott, 2002: The atmospheric bridge: The influence of ENSO teleconnections on air-sea interaction over the global ocean, *J. Climate*, **14**, 2205–2231.

Alexander, M. A., and C. Penland, 1996: Variability in a mixed layer ocean model driven by stochastic atmospheric forcing, *J. Climate*, **9**, 2424–2442.

Alexander, M. A., and J. D. Scott, 1997: Surface flux variability over the North Pacific and North Atlantic oceans, *J. Climate*, **10**, 2963–2978.

Anteneodo, C., and C. Tsallis, 2003: Multiplicative noise: A mechanism leading to nonextensive statistical mechanics, *J. Math. Phys.*, **44**, 5194–5203.

Azzalini, A., and A. Capitanio, 2003: Distributions generated by perturbations of symmetry with emphasis on a multivariate skew *t*-distribution, *J. R. Statist. Soc. B*, **65**, 367–389.

Barsugli, J. J., and D. S. Battisti, 1998: The basic effects of atmosphere-ocean thermal coupling on midlatitude variability, *J. Atmos. Sci.*, **55**, 477–493.

Blaauboer, D., G. J. Komen, and J. Reiff, 1982: The behaviour of the sea surface temperature (SST) as a response to stochastic latent- and sensible heat forcing, *Tellus*, **34**, 17–28.

Compo, G. P., P. D. Sardeshmukh, and C. Penland, 2001: Changes of subseasonal variability associated with El Niño, *J. Climate*, **14**, 3356–3374.

Diaz, H. F., C. S. Ramage, S. D. Woodruff, and T. S. Parker, 1987: *Climatic Summaries of*

Ocean Weather Ships, Tech. rep., U.S. Department of Commerce (NOAA) and University of Colorado (CIRES).

Dinsmore, R. P., 1996: Alpha, Bravo, Charlie... Ocean Weather Ships 1940-1980, *Oceanus*, **39**, 9–10.

Frankignoul, C., and K. Hasselmann, 1977: Stochastic climate models. Part II. Application to sea-surface temperature anomalies and thermocline variability, *Tellus*, **29**, 289–305.

Friedrich, R., S. Siegert, J. Peinke, S. Lück, M. Siefert, M. Lindemann, J. Raethjen, G. Deusch, and G. Pfister, 2000: Extracting model equations from experimental data, *Phys. Lett. A*, **271**, 217–222.

Gardiner, C. W., 2004: *Handbook of Stochastic Methods for Physics, Chemistry and the Natural Science, Third Edition*, Springer-Verlag, 415 pp.

Gradišek, J., S. Siegert, R. Friedrich, and I. Grabec, 2000: Analysis of time series from stochastic processes, *Phys. Rev. E*, **62**, 3146–3155.

Hall, A., and S. Manabe, 1997: Can local linear stochastic theory explain sea surface temperature and salinity variability?, *Climate Dyn.*, **13**, 167–180.

Hasselmann, K., 1976: Stochastic climate models. Part I. Theory, *Tellus*, **28**, 473–484.

Jones, M. C., and M. J. Faddy, 2003: A skew extension of the *t*-distribution, with applications, *J. R. Statist. Soc. B*, **65**, 159–174.

Kloeden, P., and E. Platen, 1992: *Numerical Solution of Stochastic Differential Equations*, Springer-Verlag, 632 pp.

Monahan, A. H., 2005: The probability distributions of sea surface wind speeds Part I: Theory and SSM/I observations, *J. Climate*, submitted.

Neelin, J. D., and W. Weng, 1999: Analytical prototypes for ocean-atmosphere interaction at midlatitudes. Part I: Coupled feedbacks as a sea surface dependent stochastic process, *J. Climate*, **12**, 2037–2049.

Newman, M., G. P. Compo, and M. A. Alexander, 2003a: ENSO-forced variability of the Pacific Decadal Oscillation, *J. Climate*, **16**, 3853–3857.

Newman, M., P. D. Sardeshmukh, C. R. Winkler, and J. S. Whitaker, 2003b: A study of subseasonal variability, *Mon. Wea. Rev.*, **31**, 1715–1732.

Paul, W., and J. Baschnagel, 1999: *Stochastic Processes: From Physics to Finance*, Springer-Verlag, 231 pp.

Peinke, J., F. Böttcher, and S. Barth, 2004: Anomalous statistics in turbulence, financial markets and other complex systems, *Ann. Phys.*, **13**, 450–460.

Penland, C., 2003a: Noise out of chaos and why it won't go away, *Bulletin of the American Meteorological Society*, **84**, 921–925.

Penland, C., 2003b: A stochastic approach to nonlinear dynamics: A review (electonic supplement to 'noise out of chaos and why it won't go away'), *Bulletin of the American Meteorological Society*, **84**, ES43–ES51.

Reynolds, R., 1978: Sea surface temperature anomalies in the North Pacific Ocean, *Tellus*, **30**, 97–103.

Ronca, R. E., and D. S. Battisti, 1997: Anomalous sea surface temperatures and local air-sea energy exchange on intraannual timescale in the northeastern subtropical Pacific, *J. Climate*, **10**, 102–117.

Sakaguchi, H., 2001: Fluctuation dissipation relation for a Langevin model with multiplicative noise, *J. Phys. Soc. Jpn.*, **70**, 3247–3250.

Sardeshmukh, P., C. Penland, and M. Newman, 2001: Rossby waves in a fluctuating medium, *Progress in Probability, Vol. 49: Stochastic Climate Models*, P. Imkeller, and J.-S. von Storch, eds., Birkhäuser Verlag, Basel.

Sardeshmukh, P. D., G. P. Compo, and C. Penland, 2000: Changes of probability associated with El Niño, *J. Climate*, **13**, 4268–4286.

Siegert, S., R. Friedrich, and J. Peinke, 1998: Analysis of data sets of stochastic systems, *Phys. Lett. A*, **243**, 275–280.

Smith, C. A., and P. D. Sardeshmukh, 2000: The effect of ENSO on the intraseasonal variance of surface temperatures in winter, *Int. J. Climatol.*, **20**, 1543–1557.

Sura, P., 2003: Stochastic analysis of Southern and Pacific Ocean sea surface winds, *J. Atmos. Sci.*, **60**, 654–666.

Sura, P., and J. J. Barsugli, 2002: A note on estimating drift and diffusion parameters from timeseries, *Phys. Lett. A*, **305**, 304–311.

Sura, P., and S. T. Gille, 2003: Interpreting wind-driven Southern Ocean variability in a stochastic framework, *J. Mar. Res.*, **61**, 313–334.

Sura, P., M. Newman, C. Penland, and P. D. Sardeshmukh, 2005: Multiplicative noise and non-Gaussianity: A paradigm for atmospheric regimes?, *J. Atmos. Sci.*, in Press.

Table 1: The Ocean Weather Stations (OWSs) used for this study.

OWS	Location	Period
P	50°N, 145° W	1949–1981
N	30°N, 140° W	1946–1974
V	34°N, 164° W	1955–1971
K	45°N, 16° W	1949–1975

Table 2: Parameters used to scale the heat flux equations for typical conditions at Ocean Weather Station P.

Air density	$\rho_A = 1.225$ Kg m^{-3}
Sea-water density	$\rho_W = 1024$ Kg m^{-3}
Mixed layer depth	$h = 50$ m
Inverse Bowen ratio	$B = 8$
Bulk transfer coefficient	$C_H = 1.5 \times 10^{-3}$
Specific heat of air	$C_a = 1004$ J Kg^{-1} K^{-1}
Specific heat of sea-water	$C_h = 4187$ J Kg^{-1} K^{-1}
Mean wind speed	$\langle \lvert\mathbf{U}\rvert \rangle = 8$ m s^{-1}
Anomalous wind speed (rms)	$\lvert\mathbf{U}\rvert' = 4$ m s^{-1}

a)

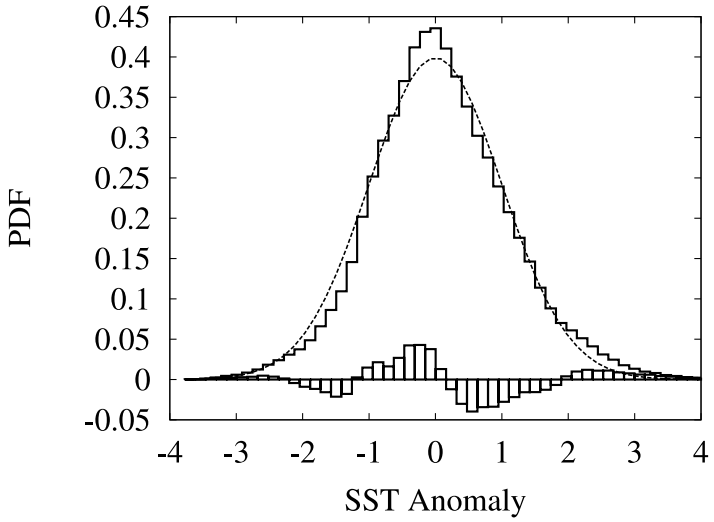

b)

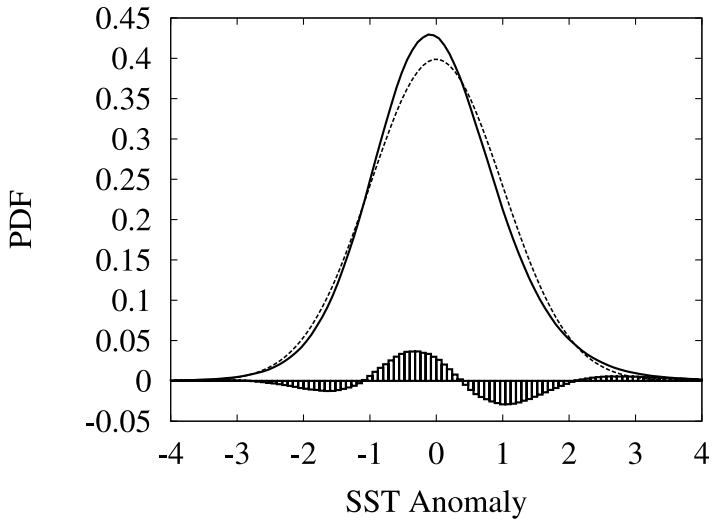

Figure 1: The PDFs of SST anomalies (in K) at OWS P, related Gaussian distributions, and deviations from Gaussianity. In (a) the PDF (steps) is calculated as a normalized histogram. The dashed line is the related Gaussian distribution, whereas the boxes denote deviations from Gaussianity. Note that the PDF has a strong peak, weak flanks, and heavy tails relative to a Gaussian distribution (the PDF is kurtosed). Furthermore, the PDF is slightly skewed. In (b) the PDF (solid line) is calculated as a MLE to a skew t-distribution. The dashed line is the related Gaussian distribution, whereas the boxes denote deviations from Gaussianity.

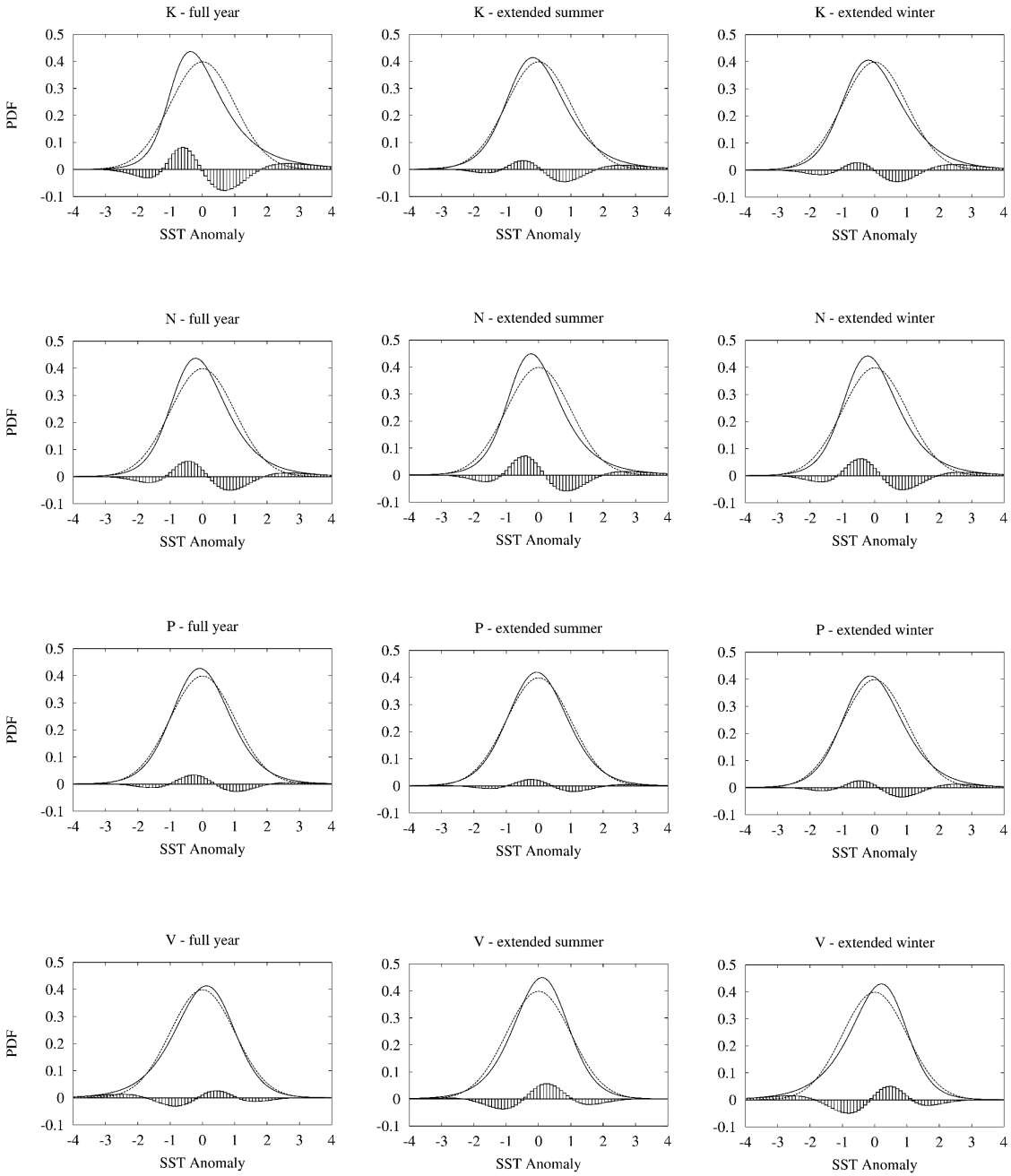

Figure 2: The PDFs of SST anomalies (normalized to make comparison possible) at locations where stochastic theory is applicable: P, N , and V in the North Pacific, and K in the North Atlantic (see Table 1 for the locations and recording periods). The PDFs (solid line) are calculated as a MLE to a skew t-distribution. The dashed lines are the related Gaussian distributions, whereas the boxes denote deviations from Gaussianity.

a)

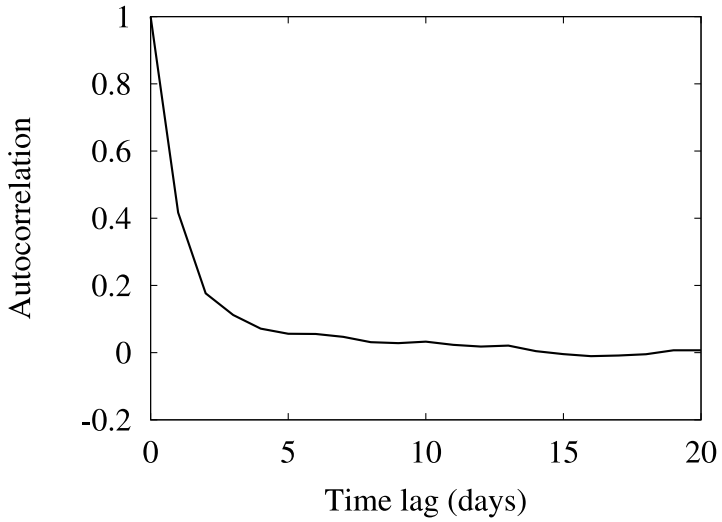

b)

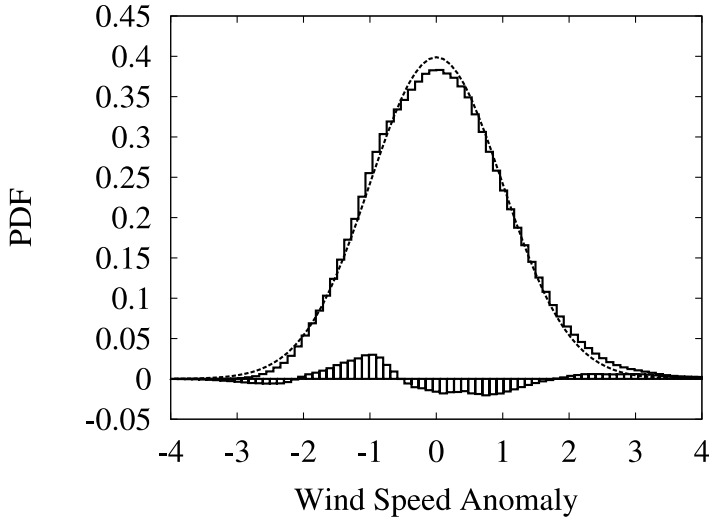

Figure 3: (a) Autocorrelation function and (b) PDF of wind speed anomalies (m/s) at OWS P.

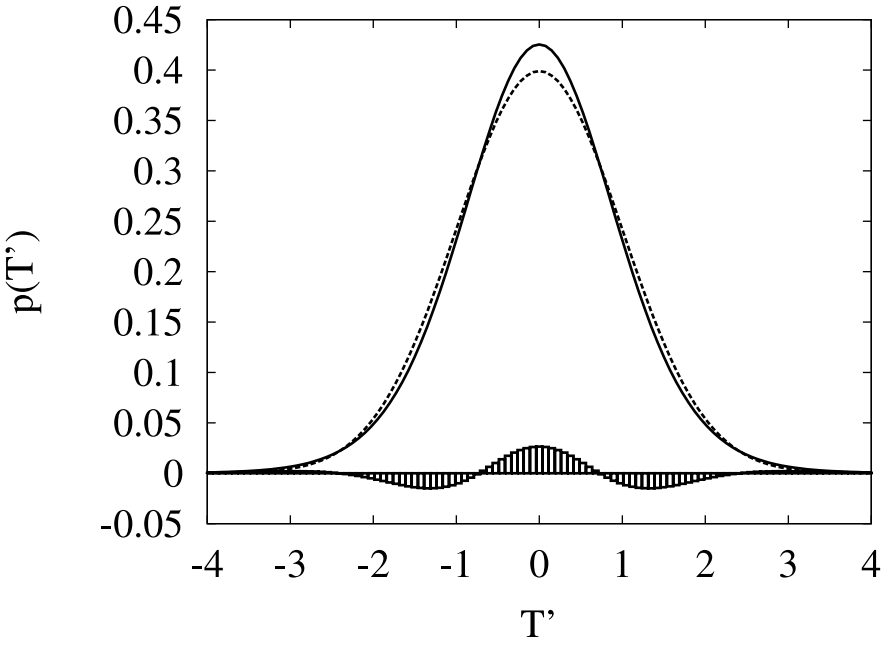

Figure 4: Stationary SST anomaly (in K) probability distributions $p(T')$ given by Eqs. (13) and (14) for $\lambda_{eff} = 0.0157$ day^{-1}, $D = 0.0104$ K^{2}day^{-1}, and $M = 0.0011$ day^{-1} together with the related Gaussian distribution and deviations from Gaussianity as in Fig. 1. Note that the general structure of the analytically derived PDF is very close to that of the observed one (Fig. 1).

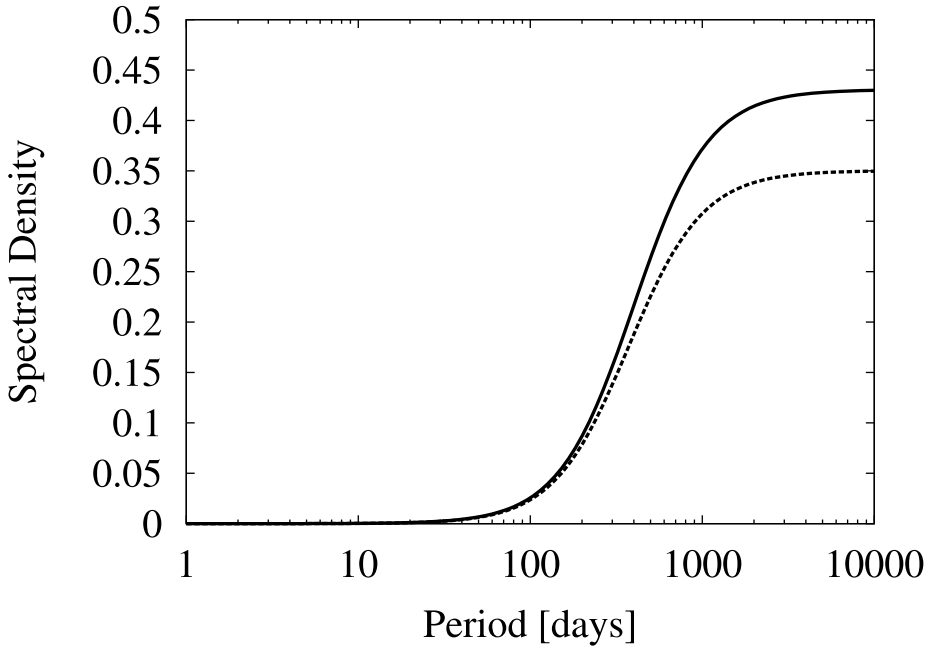

Figure 5: Spectra of linearly modeled anomalous SST variability without and with muliplicative noise given by Eq. (12). The spectrum with pure additive noise ($\lambda = 0.0168$ day^{-1}, $D = 0.0104$ K^{2}day^{-1}, and $M = 0$ day^{-1}) is indicated by the dashed line, and the spectrum with multiplicative noise ($\lambda = 0.0168$ day^{-1}, $D = 0.0104$ K^{2}day^{-1}, and $M = 0.0011$ day^{-1}) inluced is indicated by the solid line. It can be seen that the multiplicative noise enhances the low-frequency variability of anomalous SST variability by about 25% (even as the total noise variance increases only by about 8%).

a)

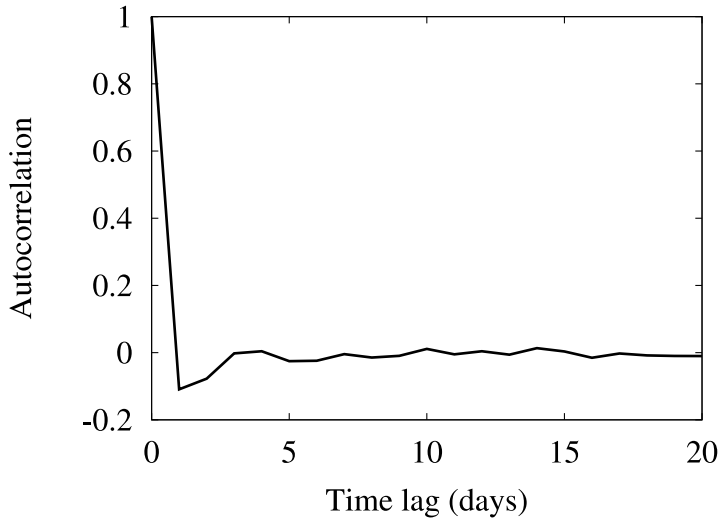

b)

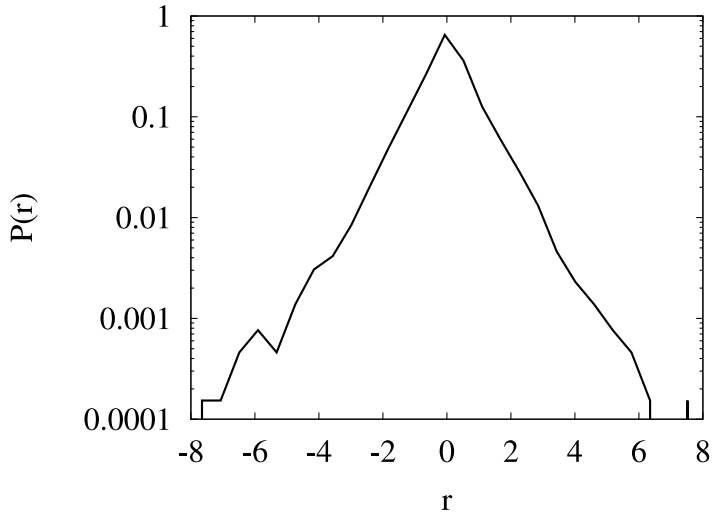

Figure 6: a) Autocorrelation function and b) PDF of the residual $r \equiv T'_{obs}(t+\Delta t) - T'(t+\Delta t)$ for the SST anomalies at OWS P. Note that the autocorrelation is close to zero after one time step (one day) and that the residual is highly non-Gaussian (very close to an exponential distribution).

a)

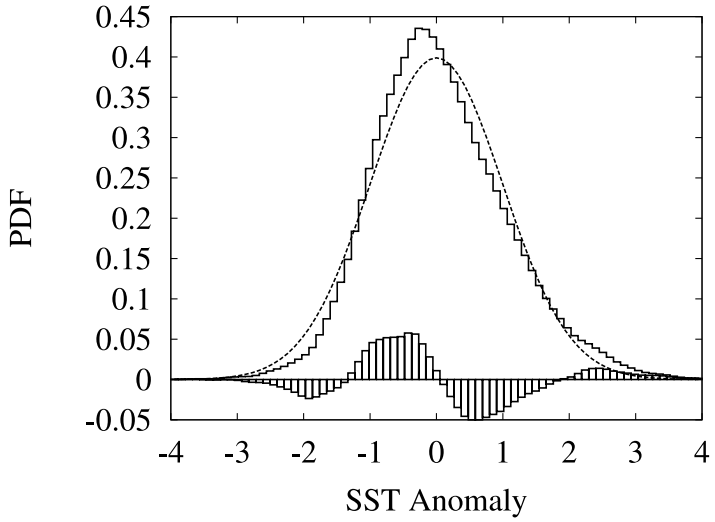

b)

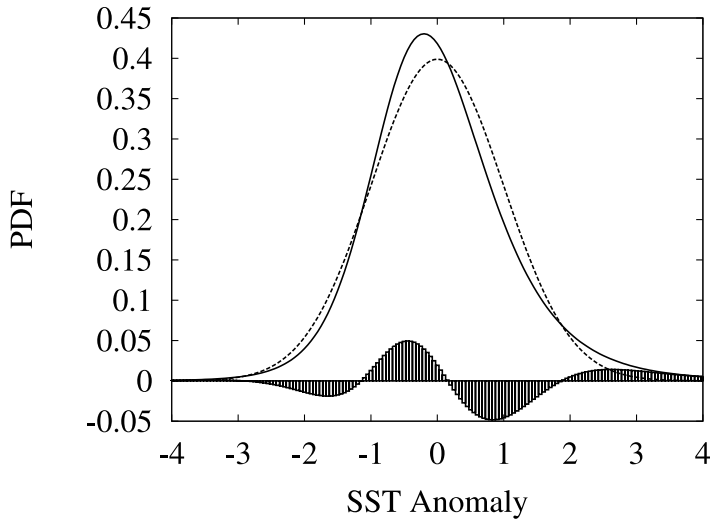

Figure 7: The PDFs of concatenated SST anomalies (nondimensional), related Gaussian distributions, and deviations from Gaussianity. In (a) the PDF (steps) is calculated as a normalized histogram. The dashed line is the related Gaussian distribution, whereas the boxes denote deviations from Gaussianity. Note that the PDF has a strong peak, weak flanks, and heavy tails relative to a Gaussian distribution (the PDF is kurtosed). Furthermore, the PDF is slightly skewed. In (b) the PDF (solid line) is calculated as a MLE to a skew t-distribution. The dashed line is the related Gaussian distribution, whereas the boxes denote deviations from Gaussianity.

a)

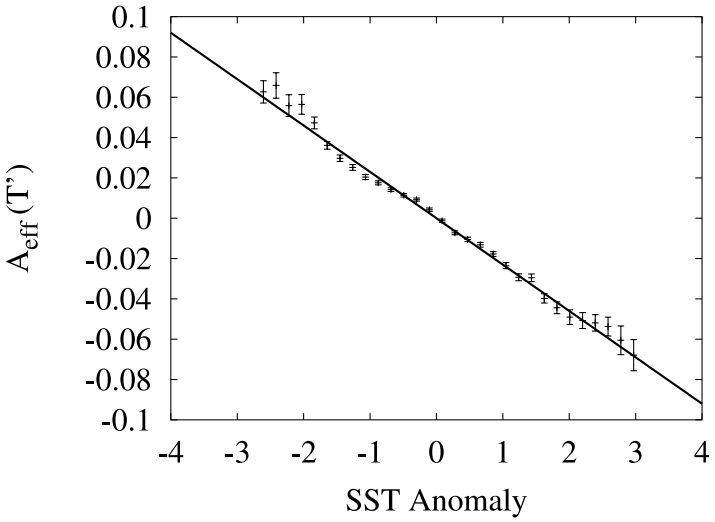

b)

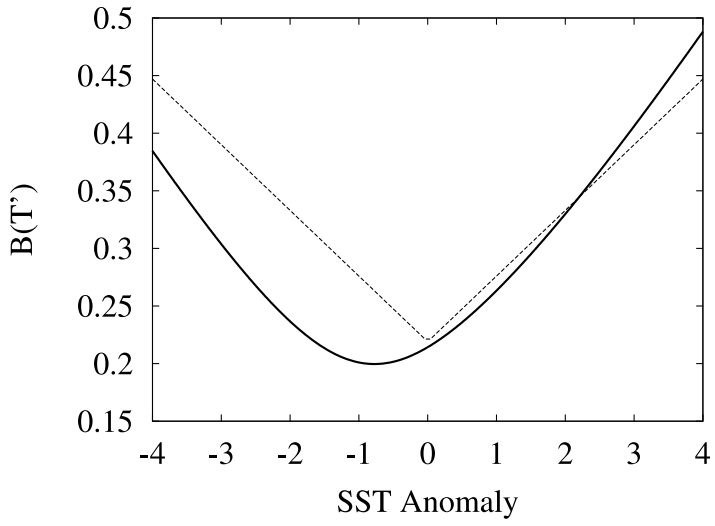

Figure 8: (a) The estimated effective drift $A_{eff}(T')$ and (b) the estimated noise $B(T')$ for the concatenated SST anomalies (nondimensional). The error bars in (a) indicate $\pm$ one standard error. The solid line in (a) shows the best linear fit. The dotted line in (b) shows the optimal linear multiplicative noise obtained by fitting the variance and the kurtosis of the PDF (Fig. 7) to the SDE (9).

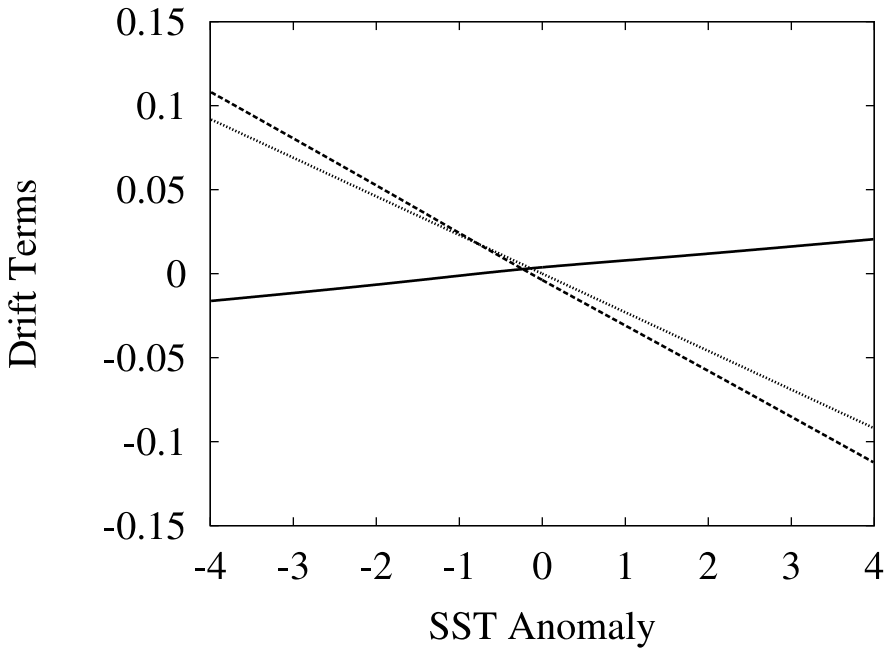

Figure 9: Noise-induced drift $1/2B(\partial B/\partial T')$ (solid line), deterministic drift A (dashed line), effective drift A_{eff} (dotted line) for the concatenated SST anomaly record.

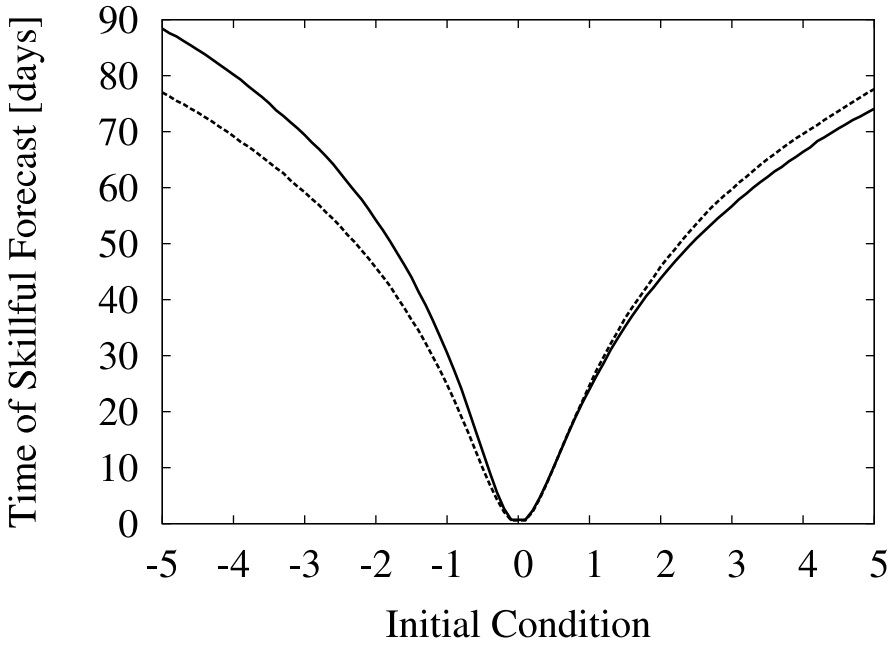

Figure 10: Time of skillful forecast (defined as $\rho_\infty = 0.5$) as a function of initial condition for the additive noise model (dashed line) and the multiplicative noise model (solid line).

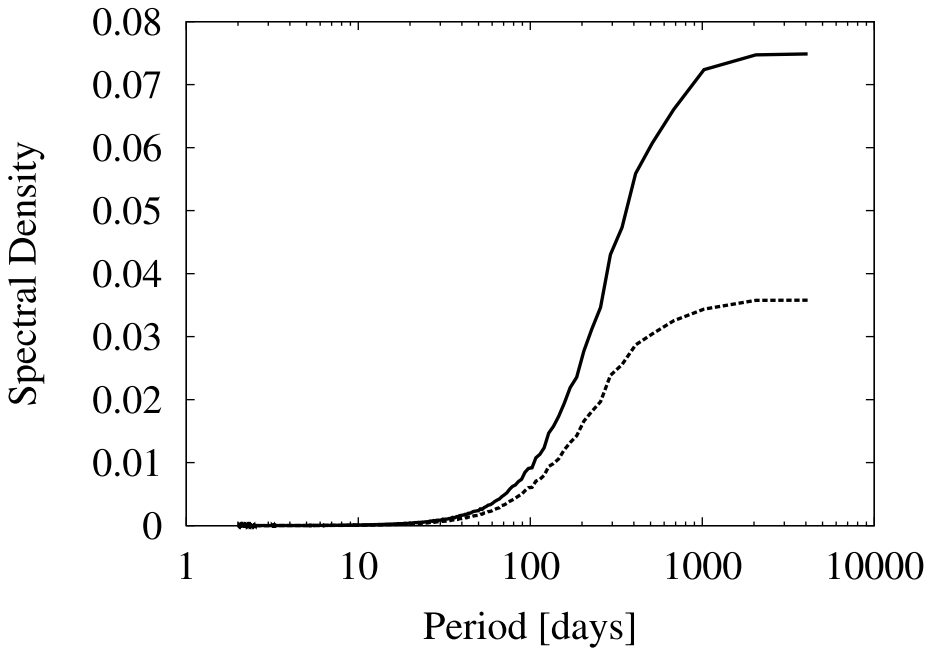

Figure 11: Spectra of nonlinearly modeled anomalous SST variability without and with muliplicative noise. The spectrum with pure additive noise is indicated by the dashed line, and the spectrum with multiplicative noise included is indicated by the solid line. It can be seen that the multiplicative noise enhances the low-frequency variability of anomalous SST variability by about 100% (even as the total noise variance increases only by about 30%).